Macromolecular Nanotechnology

# Contact angle measurements as a tool to investigate the filler–matrix interactions in polyurethane–clay nanocomposites from blocked prepolymer

Alessandro Pegoretti *, Andrea Dorigato, Marco Brugnara, Amabile Penati

*Department of Materials Engineering and Industrial Technologies, INSTM-NIPLAB Research Unit, University of Trento, via Mesiano 77, 38100 Trento, Italy*

A B S T R A C T

Optically transparent polyurethane-clay nanocomposite films were prepared by dispersing 5 wt% of various commercial organo-clays in a mixture of cycloaliphatic amines used as chain extender-cross-linker of a blocked prepolymer. For the first time, vibration-induced equilibrium contact angle measurements were successfully employed to rank the selected organo-clays accordingly to their hydrophobicity order. Polymer–clay intercalation degree in the nanocomposites, as assessed from X-ray diffraction, was strongly correlated to the water–clay equilibrium contact angle. Moreover, as the clay intercalation degree increased, a decrease of the cross-linking degree of the polyurethane matrix occured.

Uniaxial tensile tests under quasi-static and impact conditions, and isothermal thermo-gravimetric analysis were performed on both unfilled polyurethane matrix and nanocomposites. Secant tensile modulus, tensile energy to break, and thermal lifetime showed a non monotonic trend with a maximum as a function of the intercalation degree. This behaviour is discussed considering that two concomitant and contrasting effects develop as the polymer–clay intercalation degree increases: a positive improvement of the filler matrix interactions, and a negative reduction of the matrix cross-linking degree.

## 1. Introduction

Organic coatings or paints on metallic substrates give aesthetic appearance as well as protection from corrosion phenomena. The wide applicability of polyurethane (PU) coatings is mainly due to the broad selection of monomers from a huge list of macrodiols, diisocyanates, chain extenders and cross-linkers [1]. Depending on the type and amount of starting monomers, the material properties can be finely tuned as the final application requires. The history and late trends in the development of high performance polyurethane and its subclass coatings have been recently reviewed by Chattopadhyay and Raju [2].

During the last 10 years a great deal of efforts has been expended to improve the performances of elastomeric PU matrices by developing nanocomposites, mostly by the addition of organo-modified clays (organo-clays) [3–46]. In fact, following the pioneering work of Wang and Pinnavaia [4], a number of scientists investigated various methods for the production of PU-clay nanocomposites. In most cases, organo-clays have been dispersed into the polyol and the mixture was then polymerized by the addition of a diisocianate and a chain extender [9–12,21,24,28,30,41, 42,44] or of a prepolymer [29]. In other cases, organo-clays have been dispersed in the prepolymer [18,25,43,45,46], or directly in the PU matrix by solvent [5,8,13–16,22] or melt [22,26,33,45] mixing procedures. Varghese et al. [20] proposed a latex compounding route to add a pristine layered silicate (sodium hectorite) to polyurethane rubber.

Depending on the type and amount of filler, and on the level of intercalation and/or exfoliation of the clay in the PU matrix, various mechanical properties can be modified

* Corresponding author. Tel.: +39 0461 882452; fax: +39 0461 881977.
*E-mail address:* Alessandro.Pegoretti@unitn.it (A. Pegoretti).

in PU-clay nanocomposites even if the experimental results can be hardly fitted in a general scheme. For example, marked improvement in mechanical properties such as tensile modulus [4,9,14–16,22,26,33,42,43,45], tensile strength [4,10,12,16,25,26,42,43,45], tensile strain at break [4,10,12,16,24–26,43,45], storage modulus [12,15,19,20, 42,46], Shore hardness [42] and tear strength [16] have been reported by some authors. On the other hand, in some cases a reduction of tensile strength [9,15,22,25] and strain at break [9,15,22,33,42] values of the PU matrix has been reported. In some other cases, rather complex filler matrix interactions resulted in non monotonic trends of the above mechanical properties as a function of the clay type [8] and content [7,18,21,22,41]. Moreover, it has been proven that other properties such as thermal stability [5,7,13,14, 26,29,43,46,47] and gas barrier [9,14,23], can be improved by clay addition. For coating applications, the optical clarity [33,45] and corrosion protection of metallic substrates [13,43] are also very important characteristics that can be guaranteed with PU-clay nanocomposites.

Many applications, including coatings technology, require PU formulations stable at room temperature, whose polymerization or cross-linking reactions can be triggered by a temperature increase. A cured coating is then obtained by applying a layer of the coating composition to a substrate surface and heating it. Blocked polyisocyanates have proven to be highly usable for this purpose [1]. These compounds, also called end-capped or masked polyisocyanates, exploit the ability of the urethane group to be thermally decomposed. The most important masking media for isocyanate groups are phenol, caprolactam, malonate, methyl-ethyl ketoxime, isononyphenol and many others [1]. Despite the relatively large number of scientific works on PU-clay nanocomposites, only very limited informations are available on PU-clay systems obtained from blocked polyisocyanates [41,48]. Our group recently studied the industrial routes to obtain PU coatings from prepolymers blocked with methyl-ethyl ketoxime [49], and their applicability for obtaining PU-clay nanocomposites [50].

Aim of the present work is to investigate the filler–matrix interactions in a PU matrix obtained from a blocked prepolymer and filled with various organo-clays. In particular, for the first time, a measure of vibration-induced equilibrium contact angle is attempted to rank the selected organo-clays in an hydrophobicity order. The effects of the organo-clays on the mechanical and thermal properties of the resulting nanocomposites will be presented and discussed in relation to the hydrophobicity of the selected clay.

In a companion paper [51], the effect of various amounts (1, 3, 5, 7 and 10 wt%) of Cloisite® 25 A on the thermo-mechanical properties of the same PU matrix from blocked prepolymer will be presented.

## 2. Experimental

### 2.1. Materials

The polyurethane matrix used in this paper was a commercial partly cross-linked polyurethane, kindly provided by API – Applicazioni Plastiche Industriali SpA (Vicenza – Italy), based on a blocked polyurethane prepolymer. The prepolymer was obtained by MDI (2,4′ diphenylmethane-diisociananate) and a trifunctional polyether polyol (hydroxyl number 36 mgKOH/g, number average molar mass 4700 g/mol). The prepolymer had a viscosity of 110 Pa s at 20 °C and was end-capped by a methyl-ethyl ketoxime. The chain extender-cross-linker was a mixture of cycloaliphatic amines (density 0.945 g/cm³, weight average molar mass 240 g/mol, average functionality 2, viscosity at 20 °C 170 mPa s).

Natural (Cloisite® Na+) and organo-modified (Cloisite® 30B, 10A, 25A, 20A and 15A) clays were provided by Southern Clay Products, Inc. (Gonzales, Texas). Table 1 summarizes some of the characteristics of the selected organo-clays. According to the Cloisite® selection chart available on the producer web site the selected organo-clays can be ranked in the following order of increasing hydrophobicity [52]: Na+ < 30B < 10A < 25A < 20A < 15A.

### 2.2. Composites manufacturing

The selected clays were vacuum dried in an oven for 48 h at 80 °C and then mechanically dispersed in the chain extender at room temperature by using a Dispermat F1 mixer rotating at 2000 rpm for 5 min. The amount of clay was properly selected in order to achieve a 5 wt% fraction in all the investigated nanocomposites. The mixture was then ultrasonicated at room temperature in a Transsonic 460/H device at 35 kHz for 5 min. The prepolymer was added to the chain extender-clay mixture at room temperature and mechanically mixed for 5 min at 2000 rpm in the Dispermat F1. According to the producers indications, a prepolymer/chain extender ratio equal to 88/12 was adopted. The mixture was then poured on non-stick silicon paper and filmed trough a semi-automatic doctor blade device. Prepolymer unblocking and reaction with chain-extender/cross-linking agent was finally promoted by a thermal treatment at 160 °C for 2 min that generated uniform films with a thickness in the range 0.49–0.51 mm.

### 2.3. Testing procedures

#### 2.3.1. Wettability of the clays

All clay species were vacuum dried in an oven for 48 h at 80 °C. A small amount of the investigated clays was then put on a circular Teflon® sheet and inserted in the cavity of a metallic cylinder. Following a procedure originally proposed by Rogers et al. [53], a pressure of 30 MPa was applied on the clay powder with a metal plunger for 5 s at room temperature in order to obtain compact clay disks. The roughness of the compacted clay disks was determined by a Dektat 3 profilometer scanning a line 2 mm long at a sampling distance of 1 μm.

3 μl volume drops of MilliQ grade water were deposited on the clay disk with a syringe. Pictures of the drops were acquired through a digital camera positioned on a static contact angle analyzer. The acquired pictures were then analyzed with Image J 1.34S, a software developed and freely distributed by the National Institute of Health in USA, by using a plug-in purposely developed by one of

*MACROMOLECULAR NANOTECHNOLOGY*

MACROMOLECULAR NANOTECHNOLOGY

**Table 1**
Organo-clays used in this study. Information taken from the producer data sheets [52]

| Trade name | Organic modifier | Modifier concentration (meq/100 g clay) | Density (g/cm³) | $d_{001}$ spacing (nm) |
|---|---|---|---|---|
| Cloisite® Na+ | None | – | 2.86 | 1.17 |
| Cloisite® 30B | $H_3C$—$N^+$—$T$ with two $CH_2CH_2OH$ groups | 90 | 1.87 | 1.85 |
| Cloisite® 10A | $H_3C$—$N^+$—$CH_2$—(phenyl), with $CH_3$ and $HT$ | 125 | 1.90 | 1.92 |
| Cloisite® 25A | $H_3C$—$N^+$—$CH_2CHCH_2CH_2CH_2CH_3$ with $CH_3$, $HT$, and $CH_2CH_3$ | 95 | 1.87 | 1.86 |
| Cloisite® 20A | $H_3C$—$N^+$—$HT$ with $CH_3$ and $HT$ | 95 | 1.77 | 2.42 |
| Cloisite® 15A | $H_3C$—$N^+$—$HT$ with $CH_3$ and $HT$ | 125 | 1.66 | 3.15 |

Where $T$ is tallow ($\sim$65% C18; $\sim$30% C16; $\sim$5% C14) and HT is hydrogenated tallow anion: chloride.

the authors (MB) [54]. The contact angle and the drop volume calculation were performed by applying the spherical approximation of the drop. The measurement on the sessile drop as deposited from the syringe returns an advancing contact angle (see Fig. 1a). An equilibrium contact angle was measured by a vibrational method (Vibration-Induced Equilibrium Contact Angle, VIECA) [55,56]. According to this method, the supply of mechanical energy to the drop through a simple loudspeaker, allows the relaxation of the meniscus to an equilibrium shape, independently on its initial state (advancing or receding). The evolution toward an equilibrium contact angle is documented in Fig. 1b and c for a water drop on Cloisite® 15A clay disk. As documented in Fig. 1b, during the vibration process the water droplet remains symmetric, with two "fixed" points (nodal points) and it finally relaxes to an equilibrium situation. Equilibrium contact angles were measured after the sample holder vibrated for 30 s at a frequency of 230 Hz with a controlled amplitude. Only when the volume of the water droplet was steady, and so a neg-ligible absorption occurred, the equilibrium contact angle was measured. At least five measurements were performed for each experimental condition.

*2.3.2. Structure and morphology*

X-ray diffraction analyses were performed by a HRD 3000 high resolution diffractometer (Ital Structures, Italy) with a radiation wavelength of 0.1540598 nm, an initial $2\theta$ angle of 1°, and a $2\theta$ increment of 0.05°.

Digital pictures for the evaluation of the optical transparency of the specimens were collected by a Nikon Coolpix 4500 digital camera at a distance of 30 cm from the specimen.

An estimation of the cross-linking degree was performed by measuring the amount of polymer matrix that can be extracted by immersion in N,N-dimethylformamide (DMF). Specimens were immersed in DMF for 24 h, and then a thermal treatment under vacuum at 50 °C for 8 h was done, in order to remove the solvent. Measuring the mass of the specimens before ($m_b$) and after ($m_a$) the
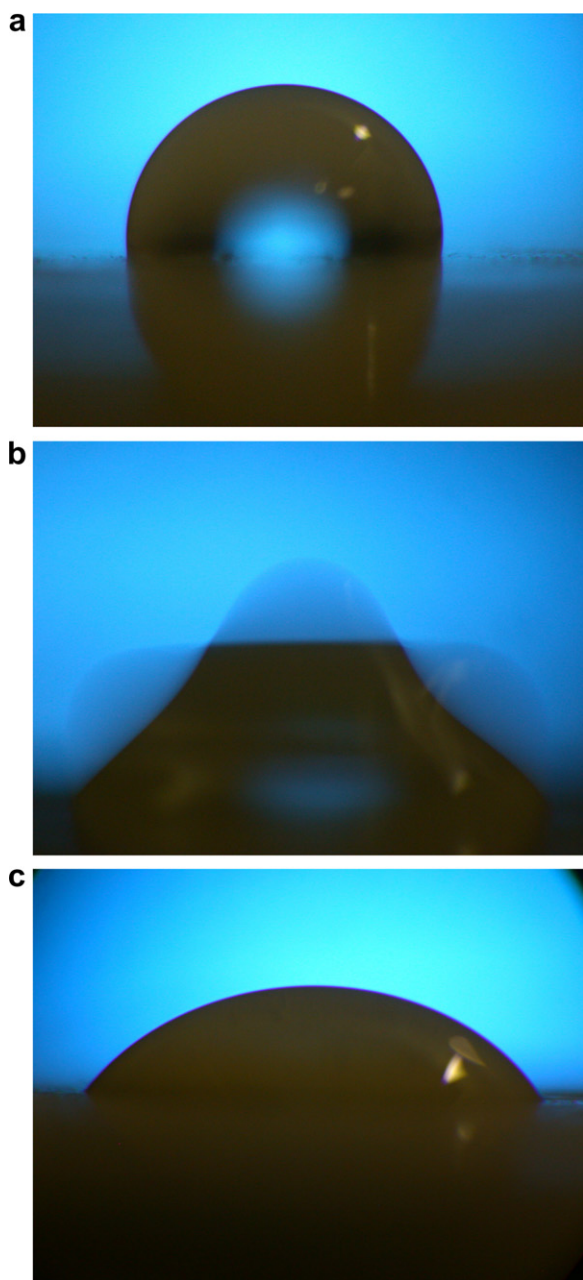
**Fig. 1.** Water droplet on a Cloisite® 15A clay disk: (a) advancing contact angle, (b) vibration-induced transition and (c) vibration-induced equilibrium contact angle.

solvent extraction procedure, a cross-linking degree (CD) was estimated as follows:

$$CD = \frac{m_a}{m_b} \quad (1)$$

### 2.3.3. Mechanical properties

Both quasi-static and impact tensile mechanical properties were measured on ISO 527 type 1BA dumbbell specimens punch cut from the polyurethane nanocomposite films. Specimens had an overall length of 74 mm and a gage width of 5 mm.

Quasi-static tensile tests were performed by an Instron model 4502 testing machine equipped with a load cell of 100 N at a cross-head speed of 50 mm/min. Axial strain was evaluated by an Instron model 2603-080 long travel extensometer for elastomers with a gage length of 25 mm. At least five specimens were tested for each sample.

Tensile impact tests were conducted by CEAST model 6549 instrumented pendulum in the tensile configuration, connected to a Ceast DAS-4000 data acquisition unit. All impact tests were performed at a striking speed of 1.0 m/s, with at a impact energy of 1.08 J, and with a sampling time of 150 ms. At least five specimens were tested for each experimental condition.

### 2.3.4. Thermal stability

Thermogravimetric analysis (TGA) was performed by a Mettler TG50 furnace, equipped with a Mettler MT5 balance connected to a Mettler TC 10A control unit. The measurements were conducted in isothermal mode, at a constant temperature of 250 °C under a nitrogen flux of 100 ml/min. A lifetime was arbitrarily estimated in correspondence of a 3 wt% mass loss.

## 3. Results and discussion

### 3.1. Contact angle measurements

The measurement of the wettability of powders is a difficult task due to the liquid absorption during the experiment. Two different approaches are proposed in the literature: (i) a wicking procedure, in which the capillary rise of the probe liquid within the specimen is modelled trough a Washburn-like equation [57,58] and (ii) the application of more common techniques (e.g. static contact angle, Wilhelmy balance) on compacted powder samples. Some criticism may be raised in both cases, but while the repeatability and the real meaning of the values obtained by the Washburn approach is not yet demonstrated [59], more congruent and physically acceptable values can be obtained on compacted powders.

The roughness of the compacted clay disks used in this work resulted in the range of $R_a$ = 0.42–0.82 mm ($R_q$ = 0.60–1.09 mm). Contact angles on "non-ideal" surfaces, such as a compacted powders, are influenced by the interfacial tensions according to Young equation, but also by many other factors, such as surface roughness [60], chemical heterogeneity [61], adsorbed layers, molecular orientation, swelling and partial solution of constituents in the material. If these effects are considered, the initial hypothesis of "ideal surface" is no longer valid. The contact angle value, where the system entails its absolute minimum of surface free energy, assumes the name of equilibrium contact angle, while the other possible contact angles correspond to different metastable equilibrium states depending on the surface and on the different initial conditions [62]. The highest of these values is commonly referred as advancing contact angle, while the lowest one

is defined as receding contact angle. The word "advancing" comes from the requirement that the drop should be just ready to spread further on the substrate surface; thus the advancing contact angle is the largest possible angle with the drop in a steady state and such an angle is more sensitive to the most hydrophobic microdomains of the surface. On the contrary, the receding contact angle is the smallest steady state angle. The static contact angle, because of the mechanism of sessile drops deposition, is an advancing angle. It follows that a comparison of the wettability of the different clays based on their static contact angle with water is clearly misleading. Only by considering the equilibrium contact angle, measured for instance by VIECA, it is possible to obtain a correct evaluation of the wettability of the sample.

Both static advancing and vibration-induced equilibrium contact angles of water on various organoclay specimens are summarized in Fig. 2. For the Cloisite® 30B clay the static advancing contact angle is $73 \pm 4°$, which is a number between the value of 60° recently measured by Malucelli et al. [63] and the value of 81° measured by Dharaya and Jana [64] for the static contact angle of water on compressed clay disks of Cloisite® 30B. On the basis of *t*-Student statistic analysis, it is possible to state that the static advancing contact angles of Cloisite® 30B, 10A, and 25A compacted clays are not statistically different, and, consequently, these clays should not differ for as concern their hydrophobicity level. On the other hand, mechanical vibrations induce a relaxation of the water droplets toward equilibrium contact angles significantly lower than the initial advancing ones. For example, the same Cloisite® 30B reaches an equilibrium contact angle of $23 \pm 1°$ after mechanical vibration. It is important to underline that the equilibrium contact angles are now statistically distinguishable, except those of Cloisite® 20A and Cloisite® 15A clays. As reported in Table 1, these two clays have the same organic modifier but in different quantities, and, consequently, a similar wettability is reasonable. Interestingly enough, the trend observed for the vibration-induced equilibrium contact angles strictly reflects the qualitative order of increasing hydrophobicity reported on the producer bul-
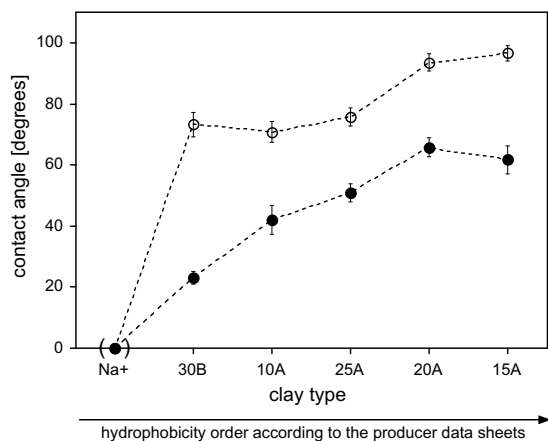
letin [52], which relies on considerations based on the chemistry and the quantity of the organic modifiers. We believe that our approach, based on the equilibrium contact angle, can provide a tool to quantify the hydrophobicity of the organo-clays in a more straightforward way. The contact angles of the pristine Na+ clay are reported under round brackets since, in this case, the water droplet was not sufficiently stable during the test (see Section 2.3.1). In fact, due to the elevated absorption from the substrate, the volume of the droplet decreased of an appreciable amount during the test. Following the same procedure, we also made an attempt to measure the equilibrium contact angles between the PU components (chain extender-cross-linker and blocked prepolymer) and the selected organo-clays. Unfortunately, due to the high viscosity of the involved chemicals compounds, the droplets were not able
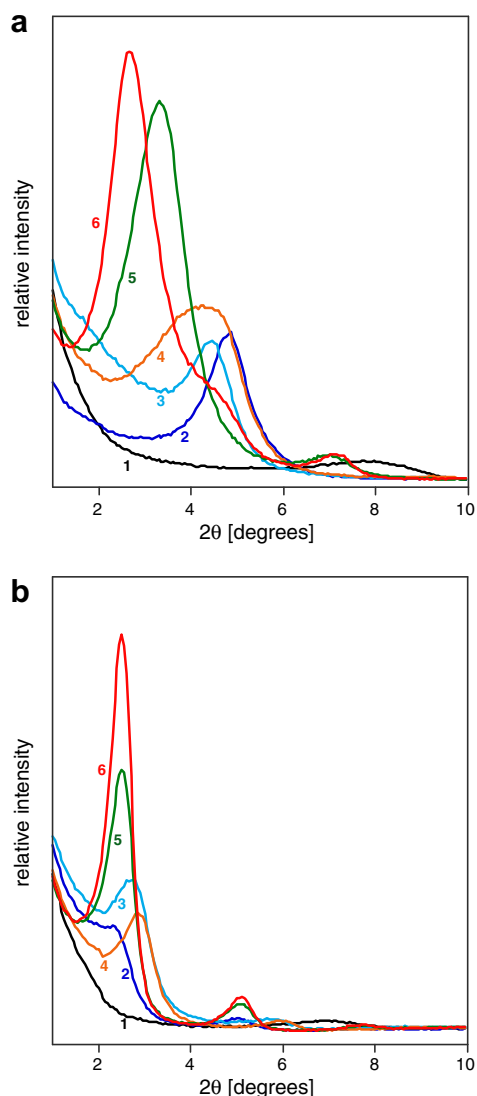
**Fig. 3.** XRD spectra collected on (a) pure clays, and (b) PU-clay nanocomposites. Numbers refer to (1) Na+, (2) 30B, (3) 10A, (4) 25A, (5) 20A, (6) 15A Cloisite® clay types.

**Fig. 2.** Static (○) and vibration-induced equilibrium (●) contact angles for various Cloisite® clays.

MACROMOLECULAR NANOTECHNOLOGY

to reach an equilibrium state on the clay surfaces. Nevertheless, since the cycloaliphatic amines chain extender-cross-linker is a highly hydrophilic liquid, its interaction with organo-clays would most probably improve as their hydrophobicity decrease, as in the case of water. From dynamic contact angle measurements (Wilhelmy balance) on a clean (oxygen plasma treated) glass sheet, the surface tension of the chain extender-cross-linker resulted equal to 32.0 mN/m, while the surface tension of the water was 72.8 mN/m. A tentative to estimate the work of adhesion between the PU matrix and the selected organo-clays is currently in progress.

### 3.2. Microstructure and morphology

X-ray diffraction patters obtained on pure clays and on PU-clay nanocomposites with 5 wt% of various Cloisite® clays are reported in Fig. 3a and b, respectively. Both natural and organo-modified clays present well defined diffraction peaks. It is worthwhile to note that, when the selected clays are incorporated into the PU matrix a shift of the characteristic peaks toward lower 2θ values can be observed. This is a clear indication that intercalation rather than exfoliation has been reached. Moreover, it is possible to observe that a small secondary peak is detectable on the XRD traces of the organo-modified clays, indicating that the ionic exchange reaction was not complete. On the basis of the Bragg's equation, the spacing of the basal plane $d_{001}$ (interlamellar distance) has been estimated and the results are summarized in Fig. 4. The interlamellar distance evaluated for the pure clays are in good accordance with the values reported on the manufacturer data sheets (see Table 1). On the basis of the $d_{001}$ spacings values, an intercalation degree (ID) parameter can be also defined as follows [65]:

$$ID = \frac{d - d_0}{d_0} \tag{2}$$

where $d$ is the interlamellar distance of the clay in the nanocomposite, and $d_0$ is the initial interlamellar distance
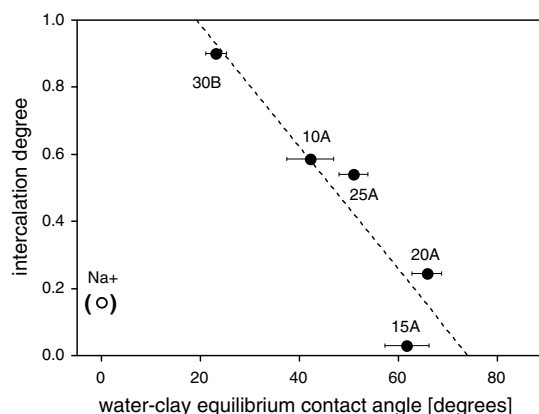


**Fig. 5.** Intercalation degree as a function of the water–clay equilibrium contact angle for various Cloisite® clay types.

in the pure clay. For all the investigated nanocomposites the ID values are reported in Fig. 5 as a function of the water–clay equilibrium contact angle. As expected, the strong interlamellar interactions and the small initial $d_{001}$ spacing of natural Na+ clay resulted in a very limited intercalation in the PU matrix, with an ID value as low as 0.16. The situation is different for as concern the organo-modified clays. In fact, it is interesting to observe that the intercalation degree markedly increases as the measured hydrophobicity (i.e. the water equilibrium contact angles) of the organo-clays decreases. This behaviour is certainly related to the highly hydrophilic nature of the chain extender-cross-linker component in which the organo-clays are initially dispersed.

Even if exfoliation is not reached, the transparency of the nanocomposites to visible light is satisfactory for coating applications, as documented in Fig. 6. A relative transparency parameter is also reported near each picture of Fig. 6. This parameter has been evaluated as the ratio between the pixels intensity on a grey scale of the printed letters located behind the specimens foils and that of the same uncovered letters (control in Fig. 6). The intensity of the grey pixels has been digitally evaluated with the aid of OriginLab®, a commercial software for scientific graphing and analysis. The relative transparency of the nanocomposites is only slightly lower than that measured for the unfilled PU matrix.

According to Eq. (1), a cross-linking degree of 0.926 has been evaluated for the unfilled PU matrix. For the PU-clay nanocomposites a relative cross-linking degree has been computed as the ratio between the CD value of the nanocomposite and that of the unfilled PU matrix. Relative cross-linking degree is reported in Fig. 7 as a function of the intercalation degree of the clay in the PU matrix. It is clearly evident that in all cases the presence of a 5 wt% of clay induces a reduction of the cross-linking degree of the PU matrix of the nanocomposites with respect to the unfilled matrix. Moreover, it is worthwhile to note that the relative cross-linking degree is decreasing as the polymer–clay intercalation increases, with a marked drop for intercalation degree values higher that 0.5. Even if the experimental techniques adopted in this work do not allow
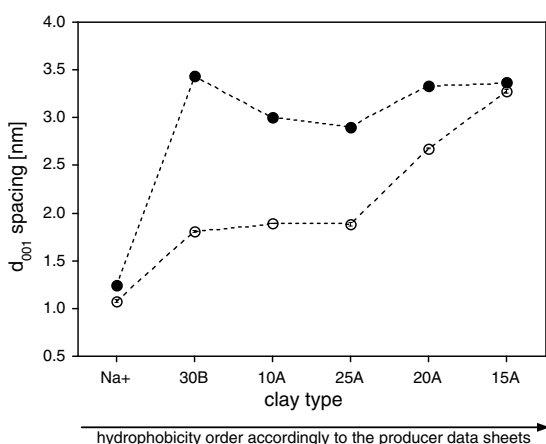


**Fig. 4.** Interlayer distance ($d_{001}$ spacing) for various Cloisite® clay types, in air (○) or dispersed in the PU matrix (●). Experimental values from X-ray diffraction analysis.

MACROMOLECULAR NANOTECHNOLOGY

Relative transparency

| | | |
|---|---|---|
| Control (uncovered letters) | TRANSPARENT | 1.000 |
| PU | TRANSPARENT | 0.872 |
| PU + 5wt% Cloisite® Na+ | TRANSPARENT | 0.825 |
| PU + 5wt% Cloisite® 30B | TRANSPARENT | 0.751 |
| PU + 5wt% Cloisite® 10A | TRANSPARENT | 0.822 |
| PU + 5wt% Cloisite® 25A | TRANSPARENT | 0.805 |
| PU + 5wt% Cloisite® 20A | TRANSPARENT | 0.799 |
| PU + 5wt% Cloisite® 15A | TRANSPARENT | 0.802 |

**Fig. 6.** Relative transparency of PU matrix and PU-clay nanocomposites.

us to fully explain this behaviour, still a couple of reasons could be hypothesized. According to the manufacturing procedure adopted in the present work, the clay is preliminary dispersed in the chain extender-cross-linker which is the component with the lower viscosity. Therefore, as the relative intercalation increases, more and more chain extender-cross-linker is probably segregated between the interlamellar galleries of the clays, where it can be hardly reached by the more viscous prepolymer. Therefore, the presence of some unreacted chain extender-cross-linker could be the reason for the lower cross-linking degree and its trend with the intercalation degree. Another possible explanation is that the thermally unblocked prepolymer may react with the hydroxyl groups [14] and/or with the counterions [47] of clays thus reducing the amount of

prepolymer available for cross-linking reactions with the chain extender-cross-linker component.

### 3.3. Mechanical behaviour

An example of the nominal stress–strain curves obtained of PU and PU-clay nanocomposite (5 wt% of Cloisite® 25A) under quasi-static and impact tensile conditions is reported in Fig. 8. Independently of the testing rate, the mechanical behaviour of the PU matrix is typically that of an elastomer in its rubbery region, and it is preserved even when 5 wt% of the selected clays is add to form the nanocomposites. As usual for elastomers, a secant modulus rather than a tangent one has been evaluated. The secant modulus at 50% strain of the unfilled PU
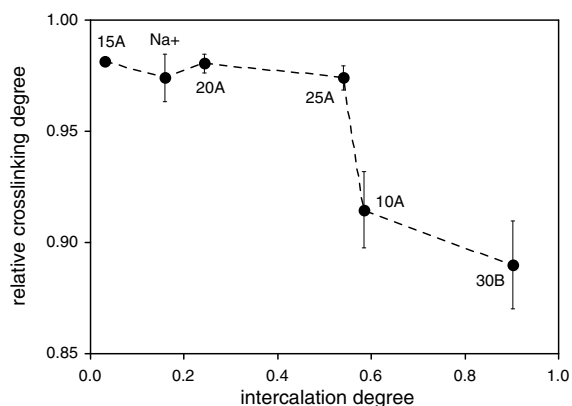
**Fig. 7.** Relative cross-linking degree as a function of the intercalation degree for various PU-clay nanocomposites.
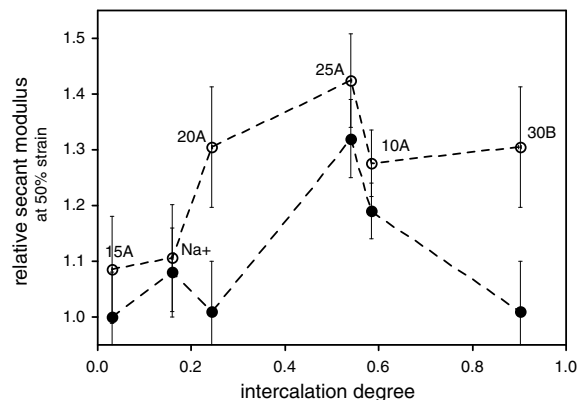


**Fig. 9.** Relative secant modulus at 50% strain under quasi-static (●) and impact (○) loading conditions as a function of the intercalation degree for various PU-clay nanocomposites.
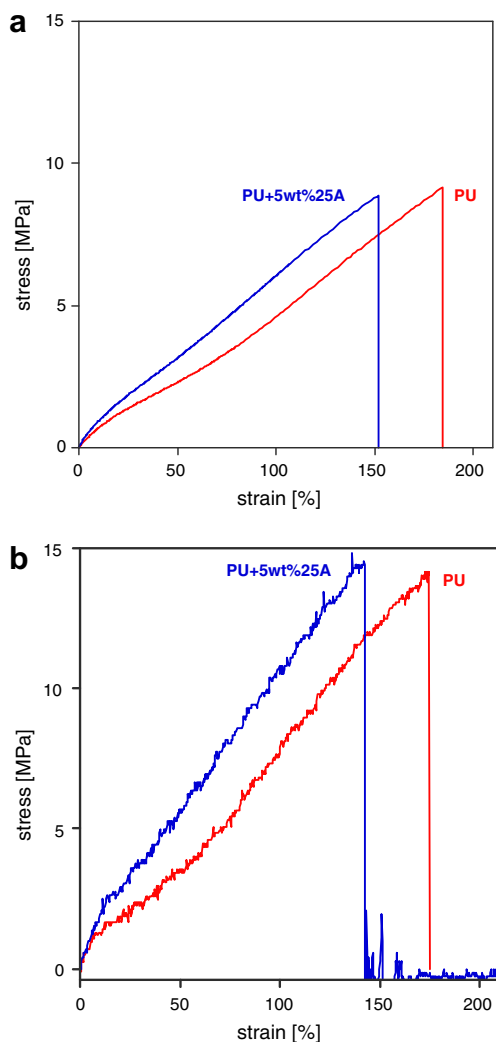


**Fig. 8.** Tensile stress–strain curves of the PU matrix (PU) and of the nanocomposite filled with 5 wt% of Cloisite® 25A clay (PU + 5 wt% 25A) under (a) quasi-static (50 mm/min) and (b) impact (1 m/s) loading conditions.

matrix is equal to 4.6 ± 0.4 MPa under quasi-static loading and to 7.5 ± 0.8 MPa under impact conditions. For both quasi-static and impact conditions, the secant modulus at 50% strain of nanocomposites filled with 5 wt% of various Cloisite® clays is reported in Fig. 9 as a relative value with respect to the unfilled PU. It can be observed that, for all the nanocomposites, secant modulus values equal to or greater than that of the unfilled PU matrix have been measured. Quite unexpectedly, the tensile secant modulus is not monotonically increasing as the intercalation degree increases. This peculiar behaviour could be tentatively explained by considering that two concomitant and concurrent phenomena occur as the polymer–clay intercalation degree increases: (i) an increasing stiffening effect related to a better dispersion of the clay in the PU matrix [14,21,33,38,43], and (ii) a reduction of the rigidity of the PU matrix due to a decrease of its cross-linking degree [66,67]. According to Fig. 7, this latter phenomenon is more pronounced for nanocomposites with intercalation degree values greater than 0.5, ie for the nanocomposites filled with Cloisite® 10A and Cloisite® 30B clays. Consistently, the tensile secant modulus of these two nanocomposites displays a discontinuity in the trend with respect to the remaining nanocomposites. As a consequence, an optimum balance between the above reported contrasting effects is reached with Cloisite® 25A clay with a relative increase of the secant modulus of 1.32 and 1.42 under quasi-static and impact conditions, respectively.

The tensile energy to break (TEB) of the unfilled PU matrix is equal to 7.7 ± 0.8 MJ/m$^3$ under quasi-static loading and to 7.2 ± 1.1 MJ/m$^3$ under impact conditions. As previously observed by other authors [9,15,22,25,33,42] a deterioration of the fracture behaviour of the PU matrix can be noticed with the incorporation of clays, as evidenced in Fig. 10 where TEB values are reported as a relative value with respect to the unfilled PU matrix. In only two cases (Cloisite® 25A and Cloisite® 10A) a slight improvement of the TEB values can be observed. It is interesting to note that, at least for the quasi-static tests even the TEB values appear to be non-monotonically related to the intercalation degree, with an optimal value for Cloisite® 25A clay.
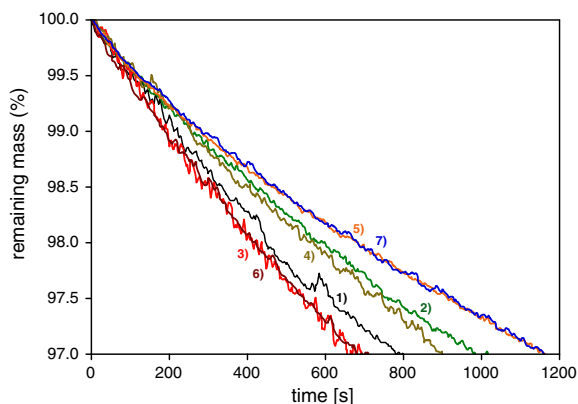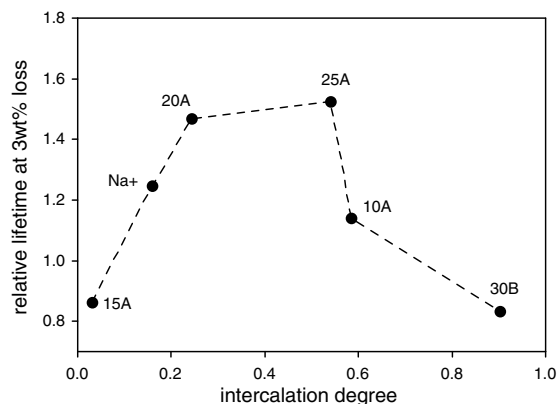
MACROMOLECULAR NANOTECHNOLOGY
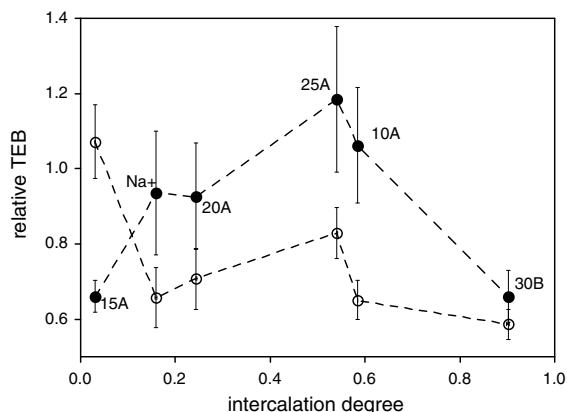
**Fig. 10.** Relative tensile energy to break (TEB) under quasi-static (●) and impact (○) loading conditions as a function of the intercalation degree for various PU-clay.



**Fig. 12.** Relative lifetime for 3 wt% mass loss as a function of the intercalation degree for various PU-clay nanocomposites.

### 3.4. Thermal stability

Isothermal thermogravimetric traces collected at 250 °C are compared in Fig. 11 for the PU matrix and the nanocomposites under investigation. As in a previous study on the thermal stability of poly(ester urethanes) [68], a lifetime is defined in relation of a given mass loss (3 wt% in this case). As evidenced in Fig. 11 the unfilled PU matrix shows a lifetime of 790 s. The lifetime of nanocomposites filled with 5 wt% of various Cloisite® clays is reported in Fig. 12 as a relative value with respect to the unfilled PU matrix. As for the mechanical properties, a non monotonic trend of the relative lifetime as a function of the intercalation degree it clearly emerges. Also this trend could be explained by supposing two concurrent and contrasting effects on the thermal stability of the nanocomposites. In fact as the intercalation degree increases an improvement of the thermal stability is generally reported [5,7,13,14,29]. On the other hand, as the intercalation degree increases a reduction of the cross-linking degree of the PU matrix occurs, which is usually associated to a lower thermal stabil-

ity [69,70]. As a consequence, similarly to the mechanical properties, an optimal balance among these two concurrent effects can be reached with Cloisite® 25A clay.

### 4. Conclusions

Vibration-induced equilibrium contact angle measurements resulted to be a powerful tool for a quantitative assessment of the hydrophobicity of a series of commercially available organo-clays.

The intercalation degree of the clays dispersed in PU matrix obtained from a blocked prepolymer resulted to be strongly related to the water–clay equilibrium contact angle of the selected organo-clays. The PU matrix cross-linking degree decreased as the clay–filler interaction improved.

Secant tensile modulus, tensile energy to break, and thermal lifetime showed a non monotonic trend as a function of the intercalation degree, showing a maximum. This behaviour was explained by considering that two concomitant and contrasting effects develop as the polymer–clay intercalation degree increases: a positive improvement of the filler matrix interactions, and a negative reduction of the matrix cross-linking degree.

**Fig. 11.** Isothermal thermogravimetric curves at 250 °C of PU matrix (1), and of nanocomposites filled with (2) Na+, (3) 30B, (4) 10A, (5) 25A, (6) 15A and (7) 20A Cloisite® clay types.

### References

[1] Schauerte K, Dahm M, Diller W, Uhlig K. Raw materials. In: Oertel G, editor. Polyurethane handbook. Munich: Hanser Publishers; 1985. p. 42–116.
[2] Chattopadhyay DK, Raju KVSN. Structural engineering of polyurethane coatings for high performance applications. Prog Polym Sci 2007;32(3):352–418.
[3] Pohl MM, Seefeld V, Mix R. TEM studies on nanocomposites of montmorillonite and polyurethane. Eur J Cell Biol 1997;74:125.
[4] Wang Z, Pinnavaia TJ. Nanolayer reinforcement of elastomeric polyurethane. Chem Mater 1998;10(12):3769–71.
[5] Chen TK, Tien YI, Wei KH. Synthesis and characterization of novel segmented polyurethane/clay nanocomposites. Polymer 2000;41(4):1345–53.

[6] Hu Y, Song L, Xu J, Yang L, Chen Z, Fan W. Synthesis of polyurethane/clay intercalated nanocomposites. Colloid Polym Sci 2001;279(8): 819–22.

[7] Ma JS, Zhang SF, Qi ZN. Synthesis and characterization of elastomeric polyurethane/clay nanocomposites. J Appl Polym Sci 2001;82(6): 1444–8.

[8] Chang JH, An YU. Nanocomposites of polyurethane with various organo-clays: thermomechanical properties, morphology, and gas permeability. J Polym Sci Part B: Polym Phys 2002;40(7):670–7.

[9] Tortora M, Gorrasi G, Vittoria V, Galli G, Ritrovati S, Chiellini E. Structural characterization and transport properties of organically modified montmorillonite/polyurethane nanocomposites. Polymer 2002;43(23):6147–57.

[10] Yao KJ, Song M, Hourston DJ, Luo DZ. Polymer/layered clay nanocomposites: 2 polyurethane nanocomposites. Polymer 2002; 43(3):1017–20.

[11] Song M, Hourston DJ, Yao KJ, Tay JKH, Ansarifar MA. High performance nanocomposites of polyurethane elastomer and organically modified layered silicate. J Appl Polym Sci 2003; 90(12):3239–43.

[12] Zhang XM, Xu RJ, Wu ZG, Zhou CX. The synthesis and characterization of polyurethane/clay nanocomposites. Polym Int 2003;52(5):790–4.

[13] Chen-Yang YW, Yang HC, Li GJ, Li YK. Thermal and anticorrosive properties of polyurethane/clay nanocomposites. J Polym Res 2004;11(4):275–83.

[14] Choi WJ, Kim SH, Kim YJ, Kim SC. Synthesis of chain-extended organifier and properties of polyurethane/clay nanocomposites. Polymer 2004;45(17):6045–57.

[15] Finnigan B, Martin D, Halley P, Truss R, Campbell K. Morphology and properties of thermoplastic polyurethane nanocomposites incorporating hydrophilic layered silicates. Polymer 2004;45(7): 2249–60.

[16] Han B, Cheng AM, Ji GD, Wu SS, Shen J. Effect of organophilic montmorillonite on polyurethane/montmorillonite nanocomposites. J Appl Polym Sci 2004;91(4):2536–42.

[17] Moon SY, Kim JK, Nah C, Lee YS. Polyurethane/montmorillonite nanocomposites prepared from crystalline polyols, using 1,4-butanediol and organo-clay hybrid as chain extenders. Eur Polym J 2004;40(8):1615–21.

[18] Ni P, Li J, Suo JS, Li SB. Novel polyether polyurethane/clay nanocomposites synthesized with organic-modified montmorillonite as chain extenders. J Appl Polym Sci 2004;94(2): 534–41.

[19] Rhoney I, Brown S, Hudson NE, Pethrick RA. Influence of processing method on the exfoliation process for organically modified clay systems. I. Polyurethanes. J Appl Polym Sci 2004;91(2):1335–43.

[20] Varghese S, Gatos KG, Apostolov AA, Karger-Kocsis J. Morphology and mechanical properties of layered silicate reinforced natural and polyurethane rubber blends produced by latex compounding. J Appl Polym Sci 2004;92(1):543–51.

[21] Xiong JW, Liu YH, Yang XH, Wang XL. Thermal and mechanical properties of polyurethane/montmorillonite nanocomposites based on a novel reactive modifier. Polym Degrad Stability 2004;86(3): 549–55.

[22] Finnigan B, Martin D, Halley P, Truss R, Campbell K. Morphology and properties of thermoplastic polyurethane composites incorporating hydrophobic layered silicates. J Appl Polym Sci 2005;97(1):300–9.

[23] Gorrasi G, Tortora M, Vittoria V. Synthesis and physical properties of layered silicates/polyurethane nanocomposites. J Polym Sci Part B: Polym Phys 2005;43(18):2454–67.

[24] Kim DS, Kim JT, Woo WB. Reaction kinetics and characteristics of polyurethane/clay nanocomposites. J Appl Polym Sci 2005;96(5): 1641–7.

[25] Pattanayak A, Jana SC. High-strength and low-stiffness composites of nanoclay-filled thermoplastic polyurethanes. Polym Eng Sci 2005;45(11):1532–9.

[26] Pattanayak A, Jana SC. Thermoplastic polyurethane nanocomposites of reactive silicate clays: effects of soft segments on properties. Polymer 2005;46(14):5183–93.

[27] Pattanayak A, Jana SC. Properties of bulk-polymerized thermoplastic polyurethane nanocomposites. Polymer 2005;46(10):3394–406.

[28] Rehab A, Salahuddin N. Nanocomposite materials based on polyurethane intercalated into montmorillonite clay. Mater Sci Eng A: Struct Mater Properties Microstruct Process 2005;399(1–2): 368–76.

[29] Song L, Hu Y, Tang Y, Zhang R, Chen ZY, Fan WC. Study on the properties of flame retardant polyurethane/organo-clay nanocomposite. Polym Degrad Stability 2005;87(1):111–6.

[30] Xia HS, Shaw SJ, Song M. Relationship between mechanical properties and exfoliation degree of clay in polyurethane nanocomposites. Polym Int 2005;54(10):1392–400.

[31] Zeng QH, Yu AB, Lu GQ. Interfacial interactions and structure of polyurethane intercalated nanocomposite. Nanotechnology 2005; 16(12):2757–63.

[32] Zha WB, Choi S, Lee KM, Han CD. Dispersion characteristics of organo-clay in nanocomposites based on end-functionalized homopolymer and block copolymer. Macromolecules 2005;38(20): 8418–29.

[33] Chavarria F, Paul DR. Morphology and properties of thermoplastic polyurethane nanocomposites: effect of organo-clay structure. Polymer 2006;47(22):7760–73.

[34] Dan CH, Lee MH, Kim YD, Min BH, Kim JH. Effect of clay modifiers on the morphology and physical properties of thermoplastic polyurethane/clay nanocomposites. Polymer 2006;47(19):6718–30.

[35] Jiang HB, Oian JW, Bai YX, Fang MH, Qian XQ. Preparation and properties of polyurethane/montmorillonite nanocomposites cured under room temperature. Polym Compos 2006;27(5):470–4.

[36] Jin J, Song M, Yao KJ, Chen L. A study on viscoelasticity of polyurethane-organo-clay nanocomposites. J Appl Polym Sci 2006; 99(6):3677–83.

[37] Wang JC, Chen YH, Wang JL. Preparation and properties of a novel elastomeric polyurethane/organic montmorillonite nanocomposite. J Appl Polym Sci 2006;99(6):3578–85.

[38] Xia HS, Song M. Intercalation and exfoliation behaviour of clay layers in branched polyol and polyurethane/clay nanocomposites. Polym Int 2006;55(2):229–35.

[39] Rehab A, Akelah A, Agag T, Shalaby N. Preparation and characterization of polyurethane-organo-clay nanocomposites. Polym Compos 2007;28(1):108–15.

[40] Xiong JW, Zheng Z, Jiang HM, Ye SF, Wang XL. Reinforcement of polyurethane composites with an organically modified montmorillonite. Compos Part A: Appl Sci Manuf 2007;38(1):132–7.

[41] Wang JC, Chen YH, Wang YQ. Preparation and characterization of novel organic montmorillonite-reinforced blocked polyurethane nanocomposites. Polymers Polym Compos 2006;14(6):591–601.

[42] Kim BK, Seo JW, Jeong HM. Morphology and properties of waterborne polyurethane/clay nanocomposites. Eur Polym J 2003;39(1):85–91.

[43] Chen-Yang YW, Lee YK, Chen YT, Wu JC. High improvement in the properties of exfoliated PU/clay nanocomposites by the alternative swelling process. Polymer 2007;48(10):2969–79.

[44] Ma XY, Lu HJ, Lian GZ, Zhao JC, Lu TL. Rectorite/thermoplastic polyurethane nanocomposites. II. Improvement of thermal and oil-resistant properties. J Appl Polym Sci 2005;96(4):1165–9.

[45] Pattanayak A, Jana SC. Synthesis of thermoplastic polyurethane nanocomposites of reactive nanoclay by bulk polymerization methods. Polymer 2005;46(10):3275–88.

[46] Tien YI, Wei KH. The effect of nano-sized silicate layers from montmorillonite on glass transition, dynamic mechanical, and thermal degradation properties of segmented polyurethane. J Appl Polym Sci 2002;86(7):1741–8.

[47] Solarski S, Benali S, Rochery M, Devaux E, Alexandre M, Monteverde F, Dubois P. Synthesis of a polyurethane/clay nanocomposite used as coating: Interactions between the counterions of clay and the isocyanate and incidence on the nanocomposite structure. J Appl Polym Sci 2005;95(2):238–44.

[48] Subramani S, Lee JM, Kim JH, Cheong IW. One-pack cross-linkable waterborne methyl ethyl ketoxime-blocked polyurethane/clay nanocomposite dispersions. Macromol Res 2005;13(5):418–26.

[49] Nicoletti G. Studio e sviluppo di intermedi poliuretanici a basso impatto ambientale. Trento: University of Trento; 2003. p. 118.

[50] Pegoretti A, Dorigato A, Penati A. Production and characterization of polyurethane-clay nanocomposites. In: Second international symposium on nanostructured and functional polymer-based materials and nanocomposites, Lyon; 2006.

[51] Dorigato A, Pegoretti A, Penati A. Effect of organo-clay content on the thermo-mechanical properties of PU-clay nanocomposites from blocked prepolymer, in press.

[52] <http://www.nanoclay.com/selection_chart.asp>. Accessed on August 2007.

[53] Rogers K, Takacs E, Thompson MR. Contact angle measurement of select compatibilizers for polymer–silicate layer nanocomposites. Polym Test 2005;24:423–7.

[54] <http://rsb.info.nih.gov/ij/plugins/contact-angle.html>. Accessed on August 2007.

[55] Della Volpe C, Brugnara M, Maniglio D, Siboni S, Wangdu T. About the possibility of experimentally measuring an equilibrium contact

MACROMOLECULAR NANOTECHNOLOGY

angle and its theoretical and practical consequences. In: Mittal K, editor. Contact angle, wettability and adhesion. Utrecht: VSP; 2006. p. 79–100.

[56] Della Volpe C, Maniglio D, Morra M, Siboni S. The determination of a 'stable-equilibrium' contact angle on heterogeneous and rough surfaces. Colloids Surfaces A: Physicochem Eng Aspects 2002; 206(1–3):47–67.

[57] Szekely J, Neumann AW, Chuang YK. The rate of capillary penetration and the applicability of the Washburn equation. J Colloid Interface Sci 1971;35:273–8.

[58] Washburn EW. The dynamics of capillary flow. Phys Rev 1921;17:374–82.

[59] Brugnara M, Degasperi E, Della Volpe C, Maniglio D, Penati A, Siboni S. Wettability of porous materials. II. Can we obtain the contact angle from the Washburn equation? In: Mittal K, editor. Contact angle, wettability and adhesion. Utrecht: VSP; 2006. p. 143–64.

[60] Wenzel RN. Resistance of solid surfaces to wetting by water. Ind Eng Chem 1936;28:988–94.

[61] Cassie ABD, Baxter S. Wettability of porous surfaces. Trans Faraday Soc 1944;40:546–51.

[62] Johnson REJ, Dettre RH. Wettability and contact angles. In: Matijevic E, editor. Surface and colloid science. New York: John Wiley; 1969. p. 85–153.

[63] Malucelli G, Ronchetti S, Lak N, Priola A, Dintcheva NT, Mantia FP. Intercalation effects in LDPE/o-montmorillonites nanocomposites. Eur Polym J 2007;43(2):328–35.

[64] Dharaiya D, Jana SC. Thermal decomposition of alkyl ammonium ions and its effects on surface polarity of organically treated nanoclay. Polymer 2005;46(23):10139–47.

[65] Pegoretti A, Dorigato A, Penati A. Tensile mechanical response of polyethylene – clay nanocomposites. Express Polym Lett 2007;1(3):123–31.

[66] Scanlan JC, Webster DC, Crain AL. Correlation between network mechanical properties and physical properties in polyester-urethane coatings. In: Film formation in Waterborne Coatings; 1996. p. 222–34.

[67] Pegoraro M, Dilandro L, Severini F, Cao N, Donzelli P. Polyurethane network structure from tensile tests. J Polym Sci Part B: Polym Phys 1991;29(3):365–70.

[68] Pegoretti A, Kolarik J, Penati A. Effect of hydrolysis on molar mass and thermal properties of poly(ester-urethanes). J Thermal Anal 1994;41:1441–52.

[69] Fambri L, Pegoretti A, Kolarik J, Gavazza C, Penati A. Thermal stabilities of different polyurethanes after hydrolytic treatment. J Thermal Anal 1998;52(3):789–97.

[70] Penczek P, Rudnik E, Arczewska B, Ostrysz R. Thermogravimetric studies of the formation and thermal-decomposition processes of cross-linked polyurethanes prepared with the use of a blocked prepolymer. Polymer 1995;40(7–8):464–7.

MACROMOLECULAR NANOTECHNOLOGY